REPORT DOCUMENTATION PAGE

Form Approved
OMB No. 0704-0188

1. REPORT DATE *(DD-MM-YYYY)*	2. REPORT DATE	3. DATES COVERED *(From - To)*
05/18/2001	Final	2/99-12/00 5/18/01

4. TITLE AND SUBTITLE

Iron and nitrate supply to Oregon coastal waters: Physical mechanisms and biological response

5a. CONTRACT NUMBER

5b. GRANT NUMBER

5c. PROGRAM ELEMENT NUMBER

6. AUTHOR(S)

Chase, Zanna; van Geen, Alexander; Kosro Michael P; Marra, John; Wheeler, Patricia A.

5d. PROJECT NUMBER

N00014-99-1-0279

5e. TASK NUMBER

5f. WORK UNIT NUMBER

7. PERFORMING ORGANIZATION NAME(S) AND ADDRESS(ES)

Lamont Doherty Earth Observatory of Columbia University
Palisades, New York 10964

8. PERFORMING ORGANIZATION REPORT NUMBER

9. SPONSORING/MONITORING AGENCY NAME(S) AND ADDRESS(ES)

Office of Naval Research
Program Officer James E. Eckman ONR 322BC
Ballston Centre Tower One
800 North Quincy Street
Arlington, VA 22217-5660

10. SPONSOR/MONITOR'S ACRONYM(S)

ONR

11. SPONSORING/MONITORING AGENCY REPORT NUMBER

12. DISTRIBUTION AVAILABILITY STATEMENT

"Approved for public release; distribution is Unlimited"

13. SUPPLEMENTARY NOTES

This work was funded by ONR and by a fellowship (awarded to Chase, Z) from the Fonds pour la Formation de Chercheurs et l'Aide a la Recherche(Quebec)

14. ABSTRACT

attached

15. SUBJECT TERMS

Sea WiFS, in-vivo fluorescence, Fast Repetition Rate Fluorometry phytoplankton biomass, coastal upwelling systems

16. SECURITY CLASSIFICATION OF:			17. LIMITATION OF ABSTRACT	18. NUMBER OF PAGES	19a. NAME OF RESPONSIBLE PERSON
a. REPORT	b. ABSTRACT	c. THIS PAGE			19b. TELEPONE NUMBER *(Include area code)*

ABSTRACT

Iron and nitrate concentrations were measured at high-resolution underway in surface waters and in vertical profiles off the Oregon coast in July, 1999. Surface Fe and N (nitrate + nitrite) concentrations measured by flow injection analysis ranged from < 0.3 to 20 nmol l^{-1} and < 0.1 to 30 μmol l^{-1}, respectively. Total dissolvable Fe concentrations, measured in unfiltered, acidified samples in surface waters and in vertical profiles, ranged from <0.3 to 300 nmol l^{-1}. Our observations indicate two dominant sources of Fe to Oregon coastal waters: Slope or shelf sediments, and the Columbia River. Sedimentary iron, largely in the particulate form, appears to be added to surface waters through wind-induced vertical mixing during strong winds; through thickening of the bottom mixed layer during relaxation or downwelling-favorable wind conditions; and by outcropping of shelf bottom-waters during upwelling events. The existence of multiple iron sources and the generally high (total) iron concentrations may explain why the distribution of phytoplankton - measured both remotely (by SeaWiFS) and underway (by *in-vivo* fluorescence) - appeared to be driven primarily by physical dynamics, and was not obviously linked to the distribution of iron. Nevertheless, at some offshore stations where underway Fe was < 0.3 nmol l^{-1}, underway measurements of the physiological state of phytoplankton by Fast Repetition Rate fluorometry were consistent with mild iron-stress.

Iron and nitrate supply to Oregon coastal waters: Physical mechanisms and biological response

Zanna Chase[1,2,5], Alexander van Geen[1], Michael P. Kosro[3], John Marra[1,4], Patricia A. Wheeler[3]

Submitted to JGR- Oceans May 18, 2001

1. Lamont-Doherty Earth Observatory of Columbia University, P.O. Box 1000, Palisades, NY 10964 USA

2. also at Department of Earth and Environmental Sciences, Columbia University

3. College of Oceanic and Atmospheric Sciences, Oregon State University, Corvallis, Oregon 97331-5503.

4. NASA Headquarters, 300 E Street SW, Room 5P33, Washington, D.C. 20546

5. Corresponding author. Now at the Monterey Bay Aquarium Research Institute,7700 Sandholdt Road, Moss Landing, CA, 95039. Email: zanna@mbari.org

GAP index terms:
4875 Trace elements, 4805 Biogeochemical cycles, 4853 Photosynthesis, 4845 Nutrients and nutrient cycling

Abstract

Iron and nitrate concentrations were measured at high-resolution underway in surface waters and in vertical profiles off the Oregon coast to determine the relationship between macro- and micro-nutrient inputs during the upwelling season. Surface Fe and N (nitrate + nitrite) concentrations measured by flow injection analysis ranged from < 0.3 to 200 nmol l^{-1} and < 0.1 to 30 µmol l^{-1}, respectively. Total dissolvable Fe concentrations, measured in unfiltered, acidified samples in surface waters and in vertical profiles, ranged from <0.3 to 300 nmol l^{-1}. Surface-water Fe and N concentrations were highly variable - and uncoupled. Our observations indicate two dominant sources of Fe to Oregon coastal waters: Slope or shelf sediments, and the Columbia River. Sedimentary iron, largely in the particulate form, appears to be added to surface waters through wind-induced vertical mixing during strong winds; through thickening of the bottom mixed layer during relaxation or downwelling-favorable wind conditions; and by outcropping of shelf bottom-waters during upwelling events. The existence of multiple iron sources and the generally high iron concentrations may explain why the distribution of phytoplankton - measured both remotely (by SeaWiFS) and underway (by *in-vivo* fluorescence) - appeared to be driven primarily by physical dynamics, and was not obviously linked to the distribution of iron. Nevertheless, at some offshore stations where underway Fe was < 0.3 nmol l^{-1}, underway measurements of the physiological state of phytoplankton by Fast Repetition Rate fluorometry were consistent with mild iron-stress.

1. Introduction

Due to their proximity to shelf sediments and terrestrial sources, coastal waters are typically enriched in iron relative to the open ocean [*Johnson et al.*, 1997]. Yet recent work in the California coastal upwelling system [*Hutchins and Bruland*, 1998; *Hutchins et al.*, 1998] has demonstrated that the addition of iron to incubation bottles from some coastal regions stimulates phytoplankton growth and nitrate consumption much as it does in open ocean high-nutrient, low-chlorophyll (HNLC) regions [e.g. *Coale et al.*, 1996]. Thus, iron is potentially an important variable controlling phytoplankton biomass and nutrient consumption in many productive coastal upwelling systems.

Most of the work to date on iron in coastal upwelling systems has focused on waters off central California [*Hutchins and Bruland*, 1998; *Hutchins et al.*, 1998; *Johnson et al.*, 1999; *Martin and Gordon*, 1988]. Dissolved iron concentrations in upwelling source-waters (depth of ~150 m, ~175 km off-shore) of the California Current are relatively low [<1 nmol l^{-1} *Martin and Gordon*, 1988], which suggests that, in contrast to its effect on the macro-nutrients, upwelling of deep water does not significantly enrich coastal waters in iron. Additional potential iron sources to the coastal ocean include shelf sediments, wind-blown dust, and riverine inputs. Given the relatively high precipitation north of central California, and the prevailing alongshore wind direction, aeolian inputs of iron are expected to be small. The concentration of dissolved iron in river water can be several orders of magnitude greater than open ocean concentrations [*Boyle et al.*, 1977]. However up to 95% of riverine filterable iron can be lost through estuarine processes such as flocculation

and precipitation [*Boyle et al.*, 1977; *Mayer*, 1982*a*], so even large rivers may contribute very little dissolved iron to the coastal ocean. Indeed, resuspended shelf sediments were found to be the dominant source of Fe to surface waters off central California, even during periods of increased river runoff [*Johnson et al.*, 1999].

The west coast of North America has considerable alongshore variability in upwelling characteristics, climate and shelf geometry, all of which could affect Fe inputs. For instance, the continental shelf off Oregon, defined by the 200 m isobath, varies from a minimum width of 11 km, just off Cape Blanco (42°N) to a maximum of 78 km, at Heceta Bank (44.2°N), and is generally wider than the shelf off California. Furthermore, in the summer, surface waters off Oregon are strongly influenced by freshwater input from the Columbia River, which has its maximum discharge in June, when the plume is directed almost exclusively southward over the Oregon shelf. The average discharge from the Columbia River at the Dalles, Oregon, in July 1999 was 7112 m^3 s^{-1} (http://waterdata.usgs.gov), which is over 10 times the discharge of the largest river in California (the Sacramento) at the same time (630 m^3 s^{-1}; California Department of Water Resources).

This paper describes high-resolution surface, and bottle-based vertical distributions of key chemical and biological properties measured off southern Oregon and northern California in July 1999. The objective is to understand the physical processes governing macro- and micro nutrient inputs during the upwelling season, and the potential impact on phytoplankton biomass and productivity. By using a physical framework defined by local winds and the velocity field we evaluate several

sources and mechanisms of iron delivery to surface waters, and their potential coupling to nitrate input.

2. Methods

2.1 Sample collection

Sampling took place off the Oregon and California coasts between July 3 and July 9, 1999 aboard the R/V *Wecoma*. Time, position, bottom depth, wind speed, downwelling solar radiation (285-2800 nm), flow-through sea surface temperature (SST) and flow-through salinity were recorded as 1-minute averages by the ship's datalogger (XMIDAS). When the ship was underway at 10 knots, a continuous stream of near-surface (~1 m depth), trace-metal clean seawater was obtained for iron and nitrate analyses using a device towed over the side of the ship, as described by van Geen *et al.* [2000]. Through its ~1 min transit from the ocean to a class-100 laminar flow bench, the pumped seawater was only in contact with Teflon®-lined tubing, with the exception of a ~50 cm length of silicone tubing (9.5 mm ID; Masterflex®) in a large peristaltic pump. All tubing was leached with 1.2 N HCl for 24 h and then rinsed thoroughly with ultra-pure MQ water (18.2 MΩ, Millipore) prior to use. The pumped flow was normally directed into a 50 ml overflowing graduated cylinder within the flow bench, from which a flow for underway iron and nitrate measurements was drawn by a peristaltic pump. By switching acid-cleaned Teflon® valves this flow was occasionally diverted to fill archive bottles for future analysis. The pumping system was turned off during CTD-intensive transects. These lines were in most cases immediately resampled after the CTD casts as a continuous transect for underway measurements.

Profile samples were collected in acid-leached high-density polypropylene bottles from Niskin bottles (General Oceanics) modified for trace metal sampling by acid leaching, replacing inner springs with c-flex tubing, and rubber o-rings with silicone o-rings. All discrete samples, including those from the underway pumping system, were acidified at sea by the addition of 1 ml l^{-1} of concentrated Seastar HCl and analyzed within 7 months by the flow injection method described below.

2.2 Flow injection analysis

Nitrate and iron were detected colorimetrically by flow-injection analysis using a 3-channel fiber-optic spectrophotometer (Ocean Optics). The sensitivity of both methods was increased with long pathlength spectrophotometric cells (LPC) using the Teflon® AF (Biogeneral) liquid core waveguide approach described by Waterbury *et al.* [1997]. A 10-port injection valve (VICI) was used to control sample and reagent flow, which permitted both the Fe and NO_3 sample loops to be filled simultaneously. A 10-port selection valve (Cheminert) was used to direct either standards or the sample stream into the system, with at least 4 standards run typically every hour. Surface seawater samples were injected every 80 seconds. Standards, run in triplicate, were mixed solutions of iron and cleaned (Chelex-100) nitrate, acidified with 1 ml l^{-1} HCl as described above for discrete samples. Nitrate was undetectable in the iron stock solution and iron was undetectable in the cleaned nitrate stock solution.

2.2.1 Iron

Iron was measured using a modification of the method of Measures *et al.* [1995], with a 10 cm LPC. We did not pre-concentrate the samples, in order to

reduce sampling time, and thereby maximize the spatial resolution of sampling, and to avoid cross-contamination in this region of strong gradients in surface Fe concentrations. To further simplify the system and minimize contamination, the sample stream was neither filtered nor acidified before injection. The lack of filtration caused clogging of the valves on several occasions in nearshore waters, which lead to system downtime. In addition to the acidified standards, unacidified MQ water (UA-MQ) was also run at every standardization. Often, the absorbance of the UA-MQ was less than that of acidified MQ water, presumably because acidified MQ was leaching some adsorbed Fe from the system. Since the seawater stream was unacidified, we subtracted the UA-MQ peak from every sample peak as a blank value and took the sensitivity (absorbance per mole Fe) from the slope of the standard curve using acidified standards. Most of the time the UA-MQ blank was not detectable above the baseline. The detection limit was ~0.3 nmol l^{-1}, based on variability of the blank. The precision, based on triplicate analyses of standards, was 1-6%. Drift over an hour separating standards, both in terms of blank and sensitivity, was generally < 20%, and was assumed to be linear as a function of time.

The same flow-injection system was used for analyzing discrete samples for iron. Five of the ports on the 10-port selection valve were dedicated to samples, and flushed thoroughly between runs. Samples containing Fe above the linear range of the method (~200 nmol l^{-1}) were diluted with acidified MQ and re-run.

Matrix effects are a concern in colorimetric trace metal analysis, especially without pre-concentration. In their development of the colorimetric method, Hirayama and Unohara [1988] found no interference from chloride, sulfate and nitrate

at concentrations up to 40 mg l^{-1}. Our standard addition experiments (not shown) found no difference between the calibration slope (absorbance per mole Fe) in acidified MQ and in low Fe seawater.

The precise chemical nature of the iron detected under these conditions is difficult to assess. The Fe measured underway in an unacidified, unfiltered stream , at a reaction pH of 6.4 for ~ 40 seconds most likely includes only the most reactive Fe, and therefore represents a minimum estimate of bioavailable Fe. Preliminary experiments using EDTA as a chelator suggest organically-bound Fe is not detected under these conditions. At the low pH (~2) of the unfiltered, stored samples, organically bound Fe, colloidal Fe, and some, if not all, particulate Fe would be certainly be released into solution during 7 months of storage. The discrete analyses may therefore be considered measurements of 'dissolvable Fe' (dFe) [*Bruland and Rue, in press*] which represents the maximum potentially bioavailable iron in the system over biologically relevant time scales.

2.2.2 Macro-nutrients

Nitrate + nitrite (N) was measured underway, as described above using the standard azo dye colorimetric method [e.g. *Anderson*, 1979]. The detection limit was 0.1 µmol l^{-1} and the precision 1-6%. N, phosphate (P) and silicic acid (Si) were measured in the lab in discrete samples from the underway pumping system by flow-injection analysis (Lachat QuikChem 8000) using standard colorimetric methods, as in [*van Geen et al.*, 2000]. Profile samples were unfiltered, unacidified, and stored frozen, and macronutrients were analyzed by standard wet chemical methods according to protocols of Gordon *et al.* [1995] using an Alpkem RFA-300.

2.3 Fluorometry

In vivo fluorescence was measured underway from the ship's flow-though intake (~3 m depth) with a Turner Designs (model 10-AU) fluorometer. The *in-vivo* fluorescence signal was calibrated with extracted chlorophyll sampled from the instrument's outlet and extracted chlorophyll from surface and 10 m Rosette samples at CTD stations, interpolated to 3 m.

The Fast Repetition Rate fluorometer (Chelsea Instruments) was run in underway mode, from the same sample stream as the underway fluorometer. We used a flash sequence of 100 saturation flashes of 1.1 μs duration, separated by ~ 2.8 μs followed by 20 relaxation flashes of 1.1 μs duration, separated by 51.6 μs. Each sample was an average of 10 sequences. Data were reduced using the Chelsea Instruments software to obtain the initial, or minimal (Fo) and maximal (Fm) fluorescence yield. From these parameters we derive the ratio Fv/Fm= (Fo-Fm)/Fm, which is the maximum change in the quantum yield of fluorescence, a quantitative measure of the efficiency of photosystem II.

3. Results

3.1 Physical setting

An image from the Advanced Very High Resolution Radiometer (AVHRR) on July 3 shows cool water nearshore throughout the study area, with the coldest waters south of Cape Blanco (43°N; Figure 1). An 8-day composite image from the Sea-viewing Wide Field-of-view Sensor (SeaWiFS) (Figure 1b) shows a clear association between cool SST in the AVHRR image and high phytoplankton biomass, despite the difference in temporal coverage between the two images (Figure 1).

South of 42°N both SST and chlorophyll occurred in distinct plumes. Many of the features of the SST and chlorophyll distributions, including a seaward extension of cool, chlorophyll-rich water south of Cape Blanco (Figure 1), can be related to the Accoustic Doppler velocity at 17 m. The surface velocity field defined the trajectory of a coastal jet, which can be followed from 45°N, where it was present nearshore, to ~44.2°N, where it began to separate from the coast, then returned shore-ward at 43°N, and finally moved offshore south of Cape Blanco (41°N), similar to the flow described by Barth *et al.* [2000] for a previous year. The flow south of 42°N is particularly energetic and complex, and is consistent with the intrusion of relatively warm, low-chlorophyll waters near the shelf-break, evident in the AVHRR and SeaWiFS images (Figure 1).

Wind vectors from three stations within the study area were broadly coherent (by inspection), and demonstrate the dominance of upwelling-favorable winds (equatorward, negative) during this season (Figure 2). However, wind-relaxation events did occur, for example at the beginning of the cruise (07/03-07/04), on 07/07 north of 43°N, and on 09/07 at 41°N (Figure 2 a,b).

3.2 Regional pattern of near-surface properties

Cape Blanco defined a boundary between two distinct regimes in SST, surface salinity and surface chlorophyll a (Figure 1 and Figure 3 a,b,c). Waters to the north of Cape Blanco, seaward of the 50 m isobath, were warm (up to 17 °C), fresh (salinity as low as 23 psu) and contained relatively little chlorophyll (< 2 $\mu g\ l^{-1}$). Upwelling centers of cool SST, high salinity and elevated chlorophyll were observed near the HH line (44°N) and north of the NH line (44.7°N), but these were restricted to within

the 200 m isobath (Figure 3). South of Cape Blanco, very cold (9 °C), salty (up to 34 psu) and chlorophyll-rich (~20 $\mu g\ l^{-1}$) waters were observed along the coast. Cool (<13 °C), salty (up to 33.5 psu), chlorophyll-rich (5-10 $\mu g\ l^{-1}$) waters extended seaward of the 1000 m isobath in this region. The very cold SSTs and high salinity measured near the CR line on 07/05 are a clear indication of strong upwelling. Winds recorded to the north and south of the CR line (42°N) at this time were indeed upwelling-favorable (Figure 2 b,c), but they were not particularly strong. This apparent discrepancy between wind and upwelling strength, as inferred from tracer distributions, can be attributed to the enhanced shoaling of the pycnocline, for a given wind stress, as a current flows cyclonically around a prominent feature, such as Cape Blanco [*Arthur*, 1965].

High concentrations of N tended to be associated with nearshore, cold, high-salinity waters (Figures 3 and 4), consistent with a primary supply from upwelling. In general there was good agreement between underway and discrete measurements of N (Figures 4a,b and 5a). The generally higher values in discrete samples could be due to acid-solubilization of particulate organic nitrogen included in the unfiltered discrete samples; some of the largest outliers were indeed from regions of high chlorophyll (Figure 5a). Some of the scatter in this relationship may also be due to smearing of signals in the underway system and the difficulty of precisely time-matching underway and discrete samples, especially in regions of strong horizontal gradients in N.

The distribution of Si, in contrast to N, was not well delimited by Cape Blanco. Si-rich waters were present both south of Cape Blanco, in the cold, salty

water along the coast near the CR line, and also north of Cape Blanco, in warm, fresh waters as far as the 1000 m isobath (Figure 3d). The presence of the Columbia River plume was indicated by the very low salinity (23-24 psu), high Si (up to 41 μmol l^{-1}) and warmer SSTs [*Park et al.*, 1972] measured offshore at the northern end of the cruise track.

Although the distributions of surface-water iron inferred from the underway and discrete measurements are similar (Figure 4), iron concentrations measured in stored, acidified samples collected from the underway pumping system were up to 20-fold higher than underway measurements by FIA (Figures 4c,d and 5b). The difference between the two measurements is greatest in shallow, near-shore waters, which are more likely to contain elevated levels of particulate Fe [*Johnson et al.*, 1997] which would be have been partly or completely solubilized by acidification. The distribution of Fe, in both the underway and discrete measurements, resembled the distribution of Si more so than the distribution of N: High Fe was observed in cold, salty waters along the coast south of Cape Blanco, and also in low salinity waters of the Columbia River plume, particularly along 45°N (Figure 4 c,d). Underway Fe concentrations were not well correlated with either salinity (Figure 6b), SST (not shown) or N (Figure 6c). Of the underway observations in this study, 55%, were of Fe <1 nmol l^{-1}, and of samples containing more than 10 μmol l^{-1} N (n=105), 20% had Fe < 0.5 nmol l^{-1}.

3.3 Vertical distributions

Selected profiles of density, N, chlorophyll *a* and dFe are shown in Figure 7. In each case, an offshore station- the upwelling source region- is paired with a near-

shore station along the same sampling line. All measurements of Fe in vertical profiles were from discrete samples (i.e., total dissolvable iron, dFe). In general, less than 20 hours separated sampling the offshore and the nearshore stations, except along the NH line, where the offshore station was sampled 4 days before the nearshore station.

The distinction between waters to the north and south of Cape Blanco is visible in the offshore density profiles, with waters north of Cape Blanco being far more stratified than those to the south (CR and EU lines) (Figure 7). The distribution of nitrate was in general related to density, presumably through isopycnal shoaling. The densest water ($\sigma_\theta = 26$) and highest nitrate (> 20 μmol l^{-1}) was found at depth at all stations, and the stations with highest surface density (NH and CR, nearshore) had the greatest surface nitrate (Figure 7). Low surface nitrate at the nearshore EU station, despite high density, suggests some consumption of N had occurred.

In contrast, the distribution of iron was not obviously related to density (Figure 7). As expected, offshore dFe concentrations were generally lower than nearshore concentrations at all depths. Although concentrations near the detection limit were measured just below the surface on the NH and FM lines, dFe concentrations greater than 10 nmol l^{-1} were observed at depth at the offshore stations on all but the NH line, with dFe > 30 nmol l^{-1} on the HH, CR and HH lines (Figure 7). These "offshore" dFe concentrations are an order of magnitude greater than those measured a similar distance from shore off Monterey Bay [*Johnson et al.*, 1999; *Martin and Gordon*, 1988].

Phytoplankton biomass, which was included in the unfiltered water samples used for Fe analysis, accounted for a small fraction of the total Fe measured in most profile samples. For example, assuming as much as 50 µgC:µgchl*a* [*Parsons et al.*, 1977] and 100 µmolFe:molC [*Sunda and Huntsman*, 1995] for coastal phytoplankton, 6 µg l^{-1} of chlorophyll *a* yields only 5 nmol l^{-1} Fe. Thus, while phytoplankton biomass could account for most of the Fe in surface waters from the offshore stations (Figure 7), it can account for at most 3% of the high dFe concentrations found near-shore, or at depth at some of the offshore stations (e.g. HH, CR and EU).

At two nearshore stations along the NH line, dFe and beam attenuation (particle concentration) had similar profile shapes, both with a mid-depth minimum (Figure 8), suggesting an association between the Fe and the particulate matter. These dFe profiles (Figure 8) resemble- in shape and magnitude- a profile reported by Martin and Gordon [1988] from a station on the inner shelf off Point Arena, CA, where they also observed similarly shaped profiles of suspended particulate matter and aluminosilicates. The most obvious explanation is that the Fe is associated with lithogenic particulate matter resuspended from sediments [*Johnson et al.*, 1999; *Martin and Gordon*, 1988]. Note that although chlorophyll (fluorescence) does not contribute significantly to dFe loads (see discussion above), it does contribute to beam attenuation [*Small and Curl*, 1968], so the presence of chlorophyll at the surface may complicate the relationships between beam attenuation, particulate matter, and Fe. We have therefore used the relationship between beam attenuation and fluorescence, derived from all CTD casts (not shown), to correct beam attenuation for the attenuation associated fluorescence. When corrected for

chlorophyll, the beam attenuation signal is reduced at the surface, but not significantly at depth (Figure 8), and the mid-depth minimum in beam attenuation is preserved. This suggests the pronounced mid-depth minimum in dFe, particularly at the station 5 km from shore, is indeed linked to the depth distribution lithogenic particles. Note that although the two stations had approximately the same 'non-chlorophyll' particle content near the surface, there was significantly less dFe at 5 km from shore than 9 km from shore (Figure 8). This may reflect either a seaward decrease in the concentration of non-particulate Fe, or a seaward decrease in the Fe content of particulate matter.

3.4 Fast Repetition Rate fluorometry

The photosynthetic competency parameter, Fv/Fm, displayed strong diel variability, with high values at night and low values during the day (Figure 9). This behavior has been observed before [e.g. *Behrenfeld and Kolber*, 1999] and is most likely caused by non-photochemical quenching at high light levels. At irradiances below 500 W m^{-2} d^{-1}, Fv/Fm decreased roughly linearly with increasing light, but there was too much scatter in this relationship for it to be used to light-correct the Fv/Fm data. We therefore restrict out analysis to FRRf measurements made between 21:00 and 05:00.

The ratio Fv/Fm reaches a maximum value of 0.65 under optimal conditions, and deviations from this ratio have been interpreted as symptomatic of physiological stress, most notably nutrient limitation [*Greene et al.*, 1994]. In the present study, nighttime Fv/Fm varied between 0.4 and 0.6, with a mean of 0.48 (Figure 10d, Table 1), suggesting a range from nutrient-replete to mildly nutrient-stressed phytoplankton. A similar range was observed on a transect between the Sargasso Sea and Delaware

Bay [*Geider et al.*, 1993a], while values of 0.25 are typical of the Fe-limited equatorial Pacific [*Behrenfeld et al.*, 1996; *Behrenfeld and Kolber*, 1999]. Although there was a trend to lower values away from the coast, at least south of 45°N (Figure 10d), no correlation was found between Fv/Fm and ambient nutrient concentrations, or between Fv/Fm and temperature or salinity (not shown).

The lowest values of nighttime Fv/Fm in this study (~0.4) were measured at stations CR7, CR8 and FM8 (Table 1). Because both dFe and Si concentrations were relatively low at these stations it is not obvious whether the low Fv/Fm reflects mild Fe-stress or mild Si-stress. Experiments with phytoplankton cultures suggest the ratios of maximal and minimum fluorescence to chlorophyll *a* - Fo/chl and Fm/chl - in dark-adapted cells should increase under Fe and NO_3 limitation [*Geider et al.*, 1993b], decrease under Si limitation [*Lippemeier et al.*, 1999], and be unaffected by P limitation [*Geider et al.*, 1993b]. We have evaluated these parameters at all sites where nighttime Fv/Fm measurements were made at CTD stations, enabling a match between average continuous FRRf parameters (while on station) and chlorophyll *a* measured in the surface Rosette sample (Table 1). Although the data are limited, the ratios Fo/chl and Fm/chl at CR7 and FM8 were the highest of any of the stations, which suggests the low Fv/Fm observed at these stations is unlikely to be due to Si limitation [*Lippemeier et al.*, 1999]. At FM8, the low N and (relatively) low dFe, low Fv/Fm and high Fo/chl are consistent with both N and Fe nutrient stress [*Geider et al.*, 1993b].

The FRR-fluorometer was run both while the ship was underway and while on station, and the value of Fv/Fm was seen to fluctuate greatly at some station

occupations. Ship drift was similar at most stations, but slightly greater along the HH line. Stations along the FM line showed the greatest temporal variability in Fv/Fm (Table 1), most notably in a region with large horizontal velocities (Figure 1). The observed Fv/Fm variability may therefore represent a Eulerian signal, with the vigorous velocity field transporting phytoplankton of variable physiological status past the sampling station. Stations along the CR line displayed the least temporal variability in Fv/Fm. Although current velocity at these CR stations was not negligible (for example, compared to the HH line), the velocity vectors suggest a recirculating circulation, which would result in local cycling of similar phytoplankton populations.

3.5 High-resolution cross-shelf transects

High resolution, underway mapping is ideally suited to the coastal upwelling environment, where small-scale spatial variability is common [*Chavez et al.*, 1991]. Here we present three cross-shelf transects of underway data that cover the sampled area and a range of upwelling conditions (TR1,TR2 and TR3; see Figures 1 and 3 for location). Discrete bottle data from the transects are reported in Table 2.

Winds were upwelling-favorable at the time of sampling TR1 (Figure 2), and the low SST, high N (up to 15 μmol l^{-1}) and high salinity near-shore indicate active upwelling (Figure 11). However, iron concentrations measured underway were low (< 0.5 nmol l^{-1}). Maximum chlorophyll was found 15 km offshore, coincident with a region of lower N, but with no corresponding change in SST or salinity (Figure 11), suggesting a removal of about 10 μmol l^{-1} N by phytoplankton growth

Transects 2 & 3 were sampled during upwelling-favorable winds following about 2 days of downwelling (Figure 2a). Near-shore SSTs along TR2 were

relatively high (14 °C) compared to SSTs further south (Figure 11), and surface-water nitrate was undetectable within about 20 km from shore (Figure 11). Thus, the surface waters at TR2 had not yet been modified after ~12 hours of upwelling-favorable local winds (Figure 6 a,b), which is consistent with previous work showing it takes about 1 day for the upwelling circulation off Oregon to respond to the wind [*Barber and Smith*, 1981; *Brink et al.*, 1994]. However, in contrast to TR1, Fe concentrations along TR2 were high within 15 km from shore. Along TR2 there was a distinct cool (11-13 °C) patch, enriched in both N and Fe (5-8 μmol l^{-1} N and ~15 nmol l^{-1} Fe) located between 20 and 30 km from shore (Figure 11). Inspection of the ADCP velocity field at 17 m and an AVHRR image from July 3 (Figure 1a) suggests this cold feature may have been advected southwestward from the region of cool SST and high N nearshore on the NH line (Figure 3c).

Waters along TR3 were influenced by the Columbia River plume, as seen by their low salinity (<31 psu; Figure 13b), and high Si (Table 2). Along TR3, in contrast to TR2, decreasing SSTs and increasing salinity, N and Fe towards the coast indicate surface waters had begun to be modified by upwelling. The contrast between the cross-shelf distribution of SST, salinity and N along TR1 and TR3 suggests upwelling was more intense (faster and from greater depth) at TR1 than at TR3, although winds were more strongly equatorward at TR3 than at TR1 at the time of sampling (Figure 6). Underway Fe was about 10 times greater all along TR3 compared to TR1, while dFe was greater nearshore at TR1, but greater offshore at TR3 (Figure 11 and Table 2). A small-scale anomaly was observed along TR3 in the

temperature and salinity data between 45 and 50 km from shore, with an enrichment of Fe and N observed at the seaward edge of this feature (Figure 11).

4. Discussion

Iron and nitrate concentrations off Oregon displayed complex spatial patterns in all dimensions. These distributions, and their correlation with biological variables, are clearly influenced by multiple factors, including topography, shelf geometry, and the magnitude and variability (spatial and temporal) of wind forcing. The following discussion focuses on mechanisms of iron inputs to the Oregon coastal region, and their biological implications.

4.1 Iron sources

The upwelling origin of surface-water nitrate is well known from previous studies of coastal upwelling systems [e.g. *Chavez et al.*, 1991; *Hayward and Venrick*, 1998] and can be seen here, for example, in the similarity between density and nitrate profiles (e.g. Figure 7). Along all sampling lines, N concentration at the nearshore station was less than or equal to the highest concentrations found in the top 200 m at the offshore station (Figure 7), which is consistent with an offshore, deep-water origin for nearshore N. In contrast to N, surface-water dFe and nearshore dFe profiles along most lines were higher than in offshore profiles, confirming the existence of iron sources distinct from the upwelling that delivers N to surface waters [*Martin and Gordon*, 1988]. Here we discuss three sources of Fe to Oregon surface waters - shelf sediments, Fe-enriched upwelling-source waters, and the Columbia River -, with an emphasis on how iron inputs relate to wind forcing, and therefore, nitrate supply (Table 3). We have no evidence to suggest a significant input of Fe from atmospheric

sources, although they may be important locally, particularly near industrial centers [*Hardy et al.*, 1985].

4.1.1 Shelf sediments

Shelf sediments have been identified as the main source of Fe to the upwelling region off central California [*Johnson et al.*, 1999]. The high Fe concentrations observed here over the broad-shelf region of Heceta Bank are an indication of the importance of sedimentary Fe sources off Oregon. However, the mechanism by which sediment-derived Fe is introduced to surface waters is not well understood. Based on our observations, we propose three such mechanisms: (1) wind mixing, (2) outcropping of the bottom boundary layer, (3) thickening of the bottom mixed layer.

Input of sedimentary Fe to surface waters through bottom-reaching, wind-induced vertical mixing is likely to be important only in non-stratified water columns, very nearshore at high wind speeds. This mode of Fe input will be coupled to N input only when strong winds are upwelling-favorable. Such conditions may have occurred nearshore at the CR line in July 1999, where a profile of dFe showed a linear increase with depth, suggesting a sedimentary source. Although winds at the time of sampling were not extremely strong (~ 7 m s^{-1} from the ship and the CARO3 lighthouse), because the water column was not stratified, wind stress may have been sufficient to resuspend bottom sediments and their associated particulate and dissolved Fe. The very low surface-water Fe measured underway at this site, in contrast to the high dFe and N values, suggests either the mixing process supplied only particulate Fe from sediments, or consumption or scavenging of dissolved Fe was very rapid.

Another way to achieve sediment-surface interaction is by increasing the thickness of the bottom mixed layer (BML, a vertically homogeneous layer above the bottom) until it intersects the surface. Sediment-rich (and therefore iron-rich), nepholoid layers are often associated with BMLs. Observations from the northern California and Oregon shelves have shown that suppressed near-bottom vertical mixing, and hence thin BMLs prevail during upwelling conditions, while enhanced vertical mixing and thick BMLs prevail during downwelling conditions [*Lentz and Trowbridge*, 1991; *Pak and Zaneveld*, 1977]. A BML develops rapidly following the onset of downwelling conditions [*Lentz and Trowbridge*, 1991; *Pak and Zaneveld*, 1977], which means even short-term wind reversals may lead to resuspension of Fe. The frequency of wind reversal events may therefore be a critical parameter in determining Fe inputs in coastal upwelling systems. This mechanism of iron input also helps explain the apparent decoupling between N and Fe distributions (e.g. Figure 6c), since it provides Fe input during wind relaxation, precisely when N inputs are minimal. Temporal variability in the height of the BML also provides one explanation for the mid-depth minimum in dFe and particle concentration profiles observed at nearshore stations on the NH line at the onset of upwelling conditions (e.g. Figure 8). Specifically, it is conceivable that during downwelling conditions, such as occurred before sampling these stations, the BML thickened and the entire water-column became turbid and iron-rich. Then with the onset of upwelling, an intermediate layer of clear, iron-poor water penetrated onto the shelf [*Lentz and Trowbridge*, 1991; *Pak and Zaneveld*, 1977].

In the absence of vertical mixing, diffusion of Fe from sediments will reach at most several cm above the sediment-water interface [*Kremling and Petersen*, 1978], and will not be easily entrained in the on-shore flow. However, recent modeling work [*Allen et al.*, 1995] and observations [*van Geen et al.*, 2000], suggest a substantial portion of upwelling flow occurs in the bottom boundary layer (BBL) and outcrops in very shallow waters near the coast. Therefore, even over steep topography (narrow shelf), some portion of a N-rich upwelling plume always interacts with the shelf where it may become enriched in Fe. Outcropping of the BBL may explain the high dFe concentrations measured very nearshore on the FM line, in N-rich, recently upwelled waters. This mechanism also provides an alternative explanation for mid-depth minimum observed in the dFe profiles at shelf stations along the NH line at the onset of upwelling (e.g. Figure 8). Namely, during intense upwelling of the BBL, high-Fe waters outcropped within several km from shore, and were then transported offshore in the surface Ekman flow, over relatively less Fe-rich waters, to produce a mid-depth minimum in dFe.

4.1.2 Enrichment of offshore waters

The work of Martin and Gordon [1988] off central California suggests that in the absence of shelf interaction, upwelling of deep offshore water cannot supply sufficient Fe to surface waters to support full consumption of the concurrently upwelled N, even if all forms of Fe are assumed to be bioavailable. Off Oregon, in contrast, we find dFe > 25 nmol l^{-1} in 4 out of 5 profiles from stations seaward of the 1000 m isobath. This is about twice the amount of Fe required to support full consumption of the ~ 25 μmol l^{-1} N present at the depth of upwelling in these source waters. The origin of these elevated levels of subsurface dFe off Oregon is not clear,

and warrants greater attention. At the FM, EU and CR lines, the increases in dFe at depth are associated with slight increases in beam attenuation (data not shown), which suggests the dFe may be largely particulate, and associated with resuspended sediment transported off the shelf [e.g. *Pak et al.*, 1980]. Another possibility is the transport of dissolved Fe from pore waters in fluidized flow along isopycnals as the result of sediment slumping [*Martin and Gordon*, 1988]. The contrast between deep dFe concentrations offshore of California and Oregon may be due in part to the presence of the Columbia River, which has an extensive influence on regional sediment characteristics [e.g. *Gross et al.*, 1967].

Regardless of its origin, iron-enrichment at mid-depth (~100 m) in offshore waters represents an important iron source to nearshore surface waters, via upwelling. This subsurface iron may also be mixed into surface waters on the outer shelf by a number of physical processes [e.g.*Chavez et al.*, 1991; *Dewey and Moum*, 1990; *Klein and Coste*, 1984; *Paduan and Niiler*, 1990]], operating on perhaps very small spatial scales. The small anomaly observed in Fe and N along TR3 may have been result of such a process, where N and Fe were brought to the surface by enhanced vertical mixing associated with the SST and salinity front, perhaps in response to wind forcing across the front [*Chavez et al.*, 1991; *Franks and Walstad*, 1997; *Klein and Coste*, 1984].

4.1.3 Columbia River

The high dFe observed as far as the 1000 m isobath in low-salinity, high-silicate water along 45°N is a strong indication that iron from the Columbia River is transported hundreds of kilometers downstream. We have not made measurements of Fe in the Columbia River itself, but a USGS program found dissolved Fe at ~200

nmol l^{-1} in July at 3 sites about 140 km upstream from the mouth [*Fuhrer et al.*, 1996], while earlier measurements of dissolved Fe in the Columbia River, compiled by Riedel et al. [1984], range from 9 to 2800 nmol l^{-1}. More data are needed, but it appears iron in the Columbia River estuary may exhibit the near-conservative behavior found in some estuaries with rapid flushing [*Mayer*, 1982*b*], rather than being lost through coagulation [*Sholkovitz et al.*, 1978].

Iron input from the Columbia River plume is important because it represents a source of iron to waters seaward of the shelf break. Furthermore, the Fe at 45°N associated with the Columbia River plume is probably in a smaller size fraction than Fe associated with resuspended sediment, since larger particles would have settled out of the plume during its ~20 day [*Huyer*, 1983] transit from the river mouth. This is consistent with the high levels of Fe measured underway in the Columbia River plume, since our underway FIA system would probably not detect iron associated with large (> colloidal) particles. Note that the presence of the Columbia River may also contribute to the shelf-sediment source of Fe by exporting Fe-rich particles accumulated in the estuary [*Mayer*, 1982*b*], or by contributing to rapid sediment accumulation and hence reducing conditions conducive to Fe flux from the sediments [*Trefry and Presley*, 1982]. River flow and hence iron inputs may vary interannually; for example, river flow in July 1999 was 36% greater than the average July flow for the past 20 years. Composite SeaWiFS images for July 1998 and July 1999 (not shown), both show high phytoplankton biomass near the mouth of the Columbia River which suggests the river, which provides iron, silicic acid and a stable surface

layer, may play an important role in maintaining biological productivity over the Oregon shelf.

4.2 Biological implications

This study was undertaken in part to evaluate whether iron might be a limiting nutrient off Oregon, as it can be in waters off central California [*Hutchins and Bruland*, 1998; *Hutchins et al.*, 1998]. Our data suggest it is not, except possibly on the outer shelf. Compared to open ocean environments and the HNLC waters observed off central California [*Hutchins and Bruland*, 1998; *Hutchins et al.*, 1998] iron concentrations- both underway and total- were high off Oregon. At these nanomolar concentrations Fe is unlikely to be limiting, even for coastal phytoplankton [*Sunda and Huntsman*, 1995]. Indeed, the relatively high (0.4-0.6) nighttime values of Fv/Fm are not consistent with severe nutrient limitation of any kind. Furthermore, the largest bloom observed in this study, south of Cape Blanco, was not coincident with the region of greatest iron inputs (over and north of Heceta Bank), but rather with the region of strongest upwelling (lowest SST, strongest shoaling of the pycnocline). However, particularly in coastal systems, the biological response to upwelling is a complex function of macro and micro-nutrient supply, light availability, seeding, acclimation, sinking and along-shore and cross-shelf transport [*Barber and Smith*, 1981]. A simple correlation between nutrient input and productivity, even on a regional scale, should therefore not be expected.

Fast Repetition Rate fluorometry (FRRf) offers an alternative to incubation experiments as a means to assess (and map) the physiological status of the phytoplankton community. The FRRf data from offshore waters along the CR line

were consistent with mild iron-stress. Note that along TR1, on the CR line, underway iron fell to below our detection limit closer to shore than did nitrate, at roughly the same distance from shore that the chlorophyll concentration fell to low levels. One interpretation of these observations is that as the near-shore phytoplankton bloom was being advected offshore in the surface Ekman layer, it came to an end about 25 km from shore due to lack of iron. The low concentrations of Si observed in this region, relative to N, may even be the result of an increased Si:N uptake ratio in Fe-stressed diatoms [*Hutchins and Bruland*, 1998; *Takeda*, 1998]. Thus, despite the relatively high iron concentrations in offshore waters of the Oregon upwelling region, our analysis of Fv/Fm and Fo/chl at CTD stations does suggest iron may exert some physiological control on the phytoplankton community. In the hierarchy of Hutchins et al [1998] these may be type 2, or "slightly Fe-stressed", communities.

From the difference between Fe concentrations measured underway and in acidified samples, and from the coherence between profiles of particle concentration and dFe, we conclude that much of the iron in the near-shore environment is associated with suspended particles. This means iron concentrations in the euphotic zone will depend critically on relative rates of solubilization of Fe from particles [e.g. *Barbeau et al.*, 1996; *Johnson et al.*, 1994; *Maranger et al.*, 1998; *Wells and Mayer*, 1991] and sinking rates of particulate Fe in the offshore-flowing surface layer. The observation that the same intensity of fluorescence-corrected beam attenuation was associated with a higher concentration of dFe near shore than offshore (e.g. Figure 8) may indicate 'stripping' of Fe from particulate phases as they move across the shelf [*Johnson et al.*, 1997]. Barber and Smith [*Barber and Smith*, 1981] have proposed

that the two-layered flow of upwelling systems makes them important sites for recycled production. The same may be true for Fe, in the sense that any particulate Fe which sinks into the BBL can be entrained in the onshore flow and reupwelled to the surface where it may be subjected to further solubilization processes.

The strong baroclinic jets of the Coastal Transition Zone (CTZ) off California do not transport a significant amount of coastally upwelled nitrate to the ocean interior [*Chavez et al.*, 1991], and this also appears to be the case off Oregon. In July 1999, N enrichment did not extend further than ~50 km from the coast (Figure 10a), even south of Cape Blanco, where the coastal jet moves offshore [*Barth et al.*, 2000]. Throughout the survey area, high dFe levels were generally restricted close to shore, but elevated levels of Fe were measured underway at all distances from shore (Figure 10 b,c), especially north of Cape Blanco, perhaps reflecting the diversity (and abundance) of iron sources. The potential for Fe export from the coastal ocean probably depends on the form of nearshore Fe. Iron that has been solubilized from lithogenic particles [*Johnson et al.*, 1997] and incorporated into the dissolved or biogenic pool may be more likely to escape sedimentation over the shelf, and be exported to the ocean interior.

5. Conclusions

The high-resolution surface water transects and vertical profiles of chemical and biological parameters presented here provide insight into the magnitude, mechanisms and consequences of iron and nitrate inputs to surface waters of the Oregon upwelling system. Our results support conclusions for central California that shelf sediments are an important source of Fe to coastal upwelling systems [*Johnson*

et al., 1999]. Sedimentary iron, largely in the particulate form, is input to surface waters through wind-induced vertical mixing, thickening of the bottom mixed layer, and upwelling through the bottom boundary layer. Off Oregon, iron input associated with the Columbia River is also important. A full description of Fe inputs to the Oregon upwelling system requires a better understanding of the magnitude, reactivity and variability of Fe inputs from the Columbia River, mid-depth waters off the Oregon shelf appear to contain significantly more total Fe than waters off central California, and this offshore enrichment also contributes Fe to surface-waters. As a result of large riverine inputs, a relatively wide shelf and offshore enrichment of deep waters, iron concentrations off Oregon, both labile and total, are generally high, and not likely to be limiting biological production. However, relatively high-nitrate (>10 μmol l^{-1} NO_3), low-iron (<0.5 nmol l^{-1}) waters do exist off Oregon, as they do off California [*Hutchins and Bruland*, 1998; *Hutchins et al.*, 1998], and this may influence phytoplankton physiology and productivity, seaward of the shelf break. The source and mechanism of iron input is expected to influence the form of iron in surface waters, its decoupling from macro-nutrients, and its residence time. Future work should characterize the biological availability of iron associated with the various input mechanisms described here.

Acknowledgements

We thank the officers and crew of the *R/V Wecoma*, who went to great lengths to assist with the underway operations. N. Ventriello and C. Ho acquired and reduced the FRRf data. J. Fleischbein kindly provided the CTD data. Discussions with J. Barth,, K. Bruland, B. Hales, R. Letelier and P. Strutton were very helpful. This work

was funded by the Office of Naval Research (NOOO14-99-1-0279 to A. van Geen) and by and a fellowship (awarded to ZC) from the Fonds pour la Formation de Chercheurs et l'Aide á la Recherche (Québec). This is LDEO publication number xxxx.

References

Allen, J.S., P.A. Newberger, and J. Federiuk, Upwelling circulation on the Oregon continental shelf 1: Response to idealized forcing, *J. Phys. Oceanogr., 25*, 1843-1866, 1995.

Anderson, L., Simultaneous spectrophotometric determination of nitrite and nitrate by flow injection analysis, *Anal. Chim. Acta, 110*, 123-128, 1979.

Arthur, R.S., On the calculation of vertical motion in eastern boundary currents from determinations of horizontal motion, *J. Geophys. Res, 70*, 2799-2803, 1965.

Barbeau, K., J.W. Moffett, D.A. Caron, P.L. Croot, and D.L. Erdner, Role of protozoan grazing in relieving iron limitation of phytoplankton, *Nature, 380*, 61-64, 1996.

Barber, R.T., and R.L. Smith, Coastal upwelling ecosystems, in *Analysis of Marine Ecosystems*, edited by A.R. Longhurst, pp. 31-68, Academic Press, New York, 1981.

Barth, J.A., S.D. Pierce, and R.L. Smith, A separating coastal upwelling jet at Cape Blanco, Oregon and its connection to the California Current System, *Deep Sea Res. II, 47*, 783-810, 2000.

Behrenfeld, M.J., A.J. Bale, Z.S. Kolber, J. Aiken, and P.G. Falkowski, Confirmation of iron limitation of phytoplankton photosynthesis in the equatorial Pacific Ocean, *Nature, 383*, 508-511, 1996.

Behrenfeld, M.J., and Z.S. Kolber, Widespread iron limitation of phytoplankton in the South Pacific Ocean, *Science, 283*, 840-843, 1999.

Boyle, E.A., J.M. Edmond, and E.R. Sholkovitz, The mechanism of iron removal in estuaries, *Geochim. Cosmochim.Acta*, *41*, 1313-1324, 1977.

Brink, K.H., J.H. Lacasce, and J.D. Irish, The effect of short-scale wind variations on shelf currents, *J. Geophys. Res*, *99*, 3305-3315, 1994.

Chavez, F.P., R.T. Barber, P.M. Kosro, A. Huyer, S.R. Ramp, T.P. Stanton, and B.R. Demendiola, Horizontal transport and the distribution of nutrients in the Coastal Transition Zone off Northern California: Effects on primary production, phytoplankton biomass and species composition, *J. Geophys. Res*, *96*, 14833-14848, 1991.

Coale, K.H., K.S. Johnson, S.E. Fitzwater, R.M. Gordon, S. Tanner, F.P. Chavez, L. Ferioli, C. Sakamoto, P. Rogers, F. Millero, P. Steinberg, P. Nightingale, D. Cooper, W.P. Cochlan, M.R. Landry, J. Constantinou, G. Rollwagen, A. Trasvina, and R. Kudela, A massive phytoplankton bloom induced by an ecosystem-scale iron fertilization experiment in the equatorial Pacific Ocean, *Nature*, *383*, 495-501, 1996.

Dewey, R.K., and J.N. Moum, Enhancement of Fronts By Vertical Mixing, *J. Geophys. Res*, *95*, 9433-9445, 1990.

Franks, P.J.S., and L.J. Walstad, Phytoplankton patches at fronts: A model of formation and response to wind events, *J. Mar. Res.*, *55*, 1-29, 1997.

Fuhrer, G., G. Tanner, J. Morace, S. McKenzie, and K. Skach, Water analysis of the lower Columbia River basin: Analysis of current and historical water-quality data through 1994., USGS, Portland, OR, 1996.

Geider, R.J., R.M. Greene, Z. Kolber, H.L. Macintyre, and P.G. Falkowski, Fluorescence assessment of the maximum quantum efficiency of photosynthesis in the western North Atlantic, *Deep-Sea Research, 40*, 1205-1224, 1993a.

Geider, R.J., J. Laroche, R.M. Greene, and M. Olaizola, Response of the photosynthetic apparatus of *Phaeodactylum Tricornutum* (Bacillariophyceae) to nitrate, phosphate, or iron starvation, *Journal of Phycology, 29*, 755-766, 1993b.

Gordon, L.I., J.C. Jennings, A.R. Ross, and J.M. Krest, A suggested protocol for continuous flow automated analysis of seawater nutrients (phosphate, nitrate, nitrite, and silicic acid) in the WOCE hydrographic program and the Joint Global Ocean Fluxes Study, Oregon State University, 1995.

Greene, R.M., Z.S. Kolber, D.G. Swift, N.W. Tindale, and P.G. Falkowski, Physiological limitation of phytoplankton photosynthesis in the eastern equatorial Pacific determined from variability in the quantum yield of fluorescence, *Limnol. Oceanogr., 39*, 1061-1074, 1994.

Gross, M.G., D.A. McManus, and H.-Y. Ling, Continental shelf sediment, Northwestern United States, *Journal of Sediment Petrology, 37*, 790-795, 1967.

Hardy, J.T., C.W. Apts, E.A. Crecelius, and N.S. Bloom, Sea-surface microlayer metal enrichments in an urban and rural bay, *Estuarine, Coastal and Shelf Science, 20*, 299-312, 1985.

Hayward, T.L., and E.L. Venrick, Nearsurface pattern in the California Current: coupling between physical and biological structure, *Deep Sea Res. II, 45*, 1617-1638, 1998.

Hirayama, K., and N. Unohara, Spectrophotometric catalytic determination of an ultratrace amount of Iron(III) in water based on the oxidation of N,N-Dimethyl-P-Phenylenediamine by hydrogen peroxide, *Anal. Chem., 60*, 2573-2577, 1988.

Hutchins, D.A., and K.W. Bruland, Iron-limited diatom growth and Si : N uptake ratios in a coastal upwelling regime, *Nature, 393*, 561-564, 1998.

Hutchins, D.A., G.R. DiTullio, Y. Zhang, and K.W. Bruland, An iron limitation mosaic in the California upwelling regime, *Limnol. Oceanogr., 43*, 1037-1054, 1998.

Huyer, A., Coastal upwelling in the California Current system, *Prog. Oceanogr., 12*, 259-284, 1983.

Johnson, K.S., F.P. Chavez, and G.E. Friederich, Continental-shelf sediment as a primary source of iron for coastal phytoplankton, *Nature, 398*, 697-700, 1999.

Johnson, K.S., K.H. Coale, V.A. Elrod, and N.W. Tindale, Iron photochemistry in seawater from the equatorial Pacific, *Mar. Chem., 46*, 319-334, 1994.

Johnson, K.S., R.M. Gordon, and K.H. Coale, What controls dissolved iron concentrations in the world ocean?, *Mar. Chem., 57*, 137-161, 1997.

Klein, P., and B. Coste, Effects of wind-stress variability on nutrient transport into the mixed layer, *Deep-Sea Research, 31*, 21-37, 1984.

Kremling, K., and H. Petersen, Distribution of Mn, Fe, Zn, Cd and Cu in Baltic seawater - A study on basis of one anchor station, *Mar. Chem.*, *6*, 155-170, 1978.

Lentz, S.J., and J.H. Trowbridge, The bottom boundary-layer over the northern California shelf, *J. Phys. Oceanogr.*, *21*, 1186-1201, 1991.

Lippemeier, S., P. Hartig, and F. Colijn, Direct impact of silicate on the photosynthetic performance of the diatom Thalassiosira weissflogii assessed by on- and off- line PAM fluorescence measurements, *J. Plankton Res.*, *21*, 269-283, 1999.

Maranger, R., D.F. Bird, and N.M. Price, Iron acquisition by photosynthetic marine phytoplankton from ingested bacteria, *Nature*, *396*, 248-251, 1998.

Martin, J.H., and R.M. Gordon, Northeast Pacific iron distributions in relation to phytoplankton productivity, *Deep-Sea Research*, *35*, 177-196, 1988.

Mayer, L.M., Aggregation of colloidal iron during estuarine mixing: Kinetics, mechanism and seasonality, *Geochim. Cosmochim.Acta*, *46*, 2527-2535, 1982a.

Mayer, L.M., Retention of riverine iron in estuaries, *Geochim. Cosmochim.Acta*, *46*, 1003-1009, 1982b.

Measures, C.I., J. Yuan, and J.A. Resing, Determination of iron in seawater by flow injection analysis using in-line preconcentration and spectrophotometric detection, *Mar. Chem.*, *50*, 3-12, 1995.

Paduan, J.D., and P.P. Niiler, A lagrangian description of motion in northern California coastal transition filaments, *J. Geophys. Res*, *95*, 18095-18109, 1990.

Pak, H., and J.R.V. Zaneveld, Bottom nepheloid layers and bottom mixed layers observed on the continental-shelf off Oregon, *J. Geophys. Res*, *82*, 3921-3931, 1977.

Pak, H., J.R.V. Zaneveld, and J. Kitchen, Intermediate nepheloid layers observed off Oregon and Washington, *J. Geophys. Res*, *85*, 6697-6708, 1980.

Park, K., C. Osterberg, and W. Forster, Chemical budget of the Columbia River, in *The Columbia River estuary and adjacent ocean waters*, edited by A. Pruter, and D. Alverson, pp. 123-135, University of Washington Press, Seattle, 1972.

Parsons, T.R., M. Takahashi, and B. Hargrave, *Biological Oceanographic Processes*, 332 pp., Pergamon, New York, 1977.

Riedel, G.F., S.L. Wilson, and R.L. Holton, Trace metals in the Columbia River estuary following the 18 May 1980 eruption of Mount St Helens, *Pacific Science*, *38*, 340-348, 1984.

Sholkovitz, E.R., E.A. Boyle, and N.B. Price, The removal of dissolved humic acids and iron during estuarine mixing, *Earth Planet. Sci. Lett.*, *40*, 130-136, 1978.

Small, L., and H. Curl, The relative contribution of particulate chlorophyll and river tripton to the extinction of light off the coast of Oregon, *Limnol. Oceanogr.*, *13*, 84-91, 1968.

Sunda, W.G., and S.A. Huntsman, Iron uptake and growth limitation in oceanic and coastal phytoplankton, *Mar. Chem.*, *50*, 189-206, 1995.

Takeda, S., Influence of iron availability on nutrient consumption ratio of diatoms in oceanic waters, *Nature*, *393*, 774-777, 1998.

Trefry, J.H., and B.J. Presley, Manganese fluxes from Mississippi delta sediments, *Geochim. Cosmochim.Acta*, *46*, 1715-1726, 1982.

van Geen, A., R.K. Takesue, J. Goddard, T. Takahashi, J.A. Barth, and R.L. Smith, Carbon and nutrient dynamics during coastal upwelling off Cape Blanco, Oregon, *Deep Sea Res. II*, *47*, 975-1002, 2000.

Waterbury, R.D., W.S. Yao, and R.H. Byrne, Long pathlength absorbance spectroscopy: trace analysis of Fe(II) using a 4.5m liquid core waveguide, *Anal. Chim. Acta*, *357*, 99-102, 1997.

Wells, M.L., and L.M. Mayer, Variations in the chemical lability of iron in estuarine, coastal and shelf waters and its implications for phytoplankton, *Mar. Chem.*, *32*, 195-210, 1991.

Tables

Table 1: Nutrient and FRRf data from CTD stations occupied at night. Surface chlorophyll *a* ($\mu g\ l^{-1}$; extracted, not estimated from *in-vivo* fluorescence), macronutrients ($\mu mol\ l^{-1}$), dissolvable iron (dFe, $nmol\ l^{-1}$) and photosynthetic parameters (measured by the underway FRRf). FRRf data acquired every 4 minutes were averaged over each station occupation. The dFe value at all stations except CR7 and CR9 is from discrete surface samples collected at station locations during underway transits.

Station	Lat. °N	Lon. °W	Chl *a*	Si	P	N	dFe	Fo/chl	Fm/chl	Fv/Fm	stdev[a] Fv/Fm
CR 7	41.90	-125.00	2.08	< 0.2	0.5	3.0	1.5	276.6	462.5	0.40	0.03
CR 8	41.90	-125.20		< 0.2	0.7	2.7	3.1			0.40	0.02
CR 9	41.90	-125.33	4.95	2.2	0.8	8.0	3.9	134.6	280.1	0.52	0.02
FM 5	43.22	-124.67	0.77	3.0	< 0.1	< 0.1	8.4	184.8	363.3	0.49	0.07
FM 6	43.22	-124.75								0.55	0.12
FM 7	43.22	-124.83	0.40	3.0	< 0.1	< 0.1	3.2	208.0	364.6	0.43	0.07
FM 8	43.22	-125.00	0.32	0.2	< 0.1	< 0.1	1.9	240.8	391.2	0.39	0.05
HH 3	44.00	-124.60		3.5	0.1	< 0.1	19.6			0.51	0.05
HH 4	44.00	-124.80	0.71	2.9	< 0.1	< 0.1	10.7	132.3	248.6	0.47	0.05
HH 5	44.00	-125.00	0.90	3.0	< 0.1	< 0.1	4.1	106.8	233.2	0.54	0.05
HH 6	44.00	-125.10								0.55	0.06

a. Standard deviation of Fv/Fm during first 40 minutes on station

Table 2: Discrete nutrient analyses from along the high-resolution underway transects presented in Figure 11.

Transect	Lat. °N	Lon. °W	Distance km	P (μmol l^{-1})	Si (μmol l^{-1})	N (μmol l^{-1})	dFe (nmol l^{-1})
TR1							
	41.90	-124.65	49.7	0.4	1.2	0.1	< 0.3
	41.90	-124.58	41.9	0.5	< 0.2	2.6	< 0.3
	41.90	-124.53	35.4	0.6	< 0.2	3.3	< 0.3
	41.90	-124.43	25.2	1.1	10.9	11.3	0.7
	41.90	-124.38	19.1	1.1	18.5	11.1	58.4
	41.90	-124.32	12.2	1.6	32.0	18.1	117.0
TR2	44.01	-124.19	6.1	0.3	2.5	< 0.1	194.9
	44.05	-124.24	11.6	0.3	0.2	0.3	27.5
	44.09	-124.29	17.5	0.3	4.5	1.4	13.2
	44.13	-124.33	22.9	0.7	10.3	6.3	9.3
	44.19	-124.41	32.6	0.1	1.9	< 0.1	44.0
TR3	44.87	-124.28	26.4	0.13	6.37	1.49	28.0
	44.73	-124.52	50.9	0.10	5.88	< 0.1	31.9
	44.65	-124.65	72.2	0.10	8.35	< 0.1	36.1

Table 3: Proposed sources and mechanisms of iron inputs to surface waters and their relationship to nitrate input.

Iron source	Mechanism	Winds	Nitrate input
Shelf sediments	wind-induced mixing	strong; equatorward or poleward	No
	thickening of bottom mixed layer/ bottom nepheloid layer	weak or poleward	No
	outcropping of the bottom boundary layer	strong; equatorward	Yes
Offshore deepwater	isopycnal shoaling; diapycnal vertical mixing	strong; equatorward	Yes
Columbia River	plume transport	any	small

Figure legends

Figure 1: ADCP velocity vectors (longest arrow represents 42 cm/s) at 17 m between 3-8 July 1999 overlaid on satellite-derived (a) sea surface temperature (°C) from 5 July and (b) an 8-day (7/4-7/11) composite of satellite-derived chlorophyll *a* concentration ($\mu g\ l^{-1}$). Chlorophyll is displayed on a logarithmic scale. There is no chlorophyll data in the black regions near the coast. A probable path of the coastal current has been subjectively drawn through the velocity vectors in (a). The location of three transects where high-resolution data are examined more closely are also indicated in (a). Initials along the coast indicate the standard sampling lines of the Oregon GLOBEC program.

Figure 2: Wind vectors ($m\ s^{-1}$) measured from (a) near the NH line at the Newport buoy (44.6°N, 124.5°W; NOAA buoy no. 46050), (b) near the FM line at the Cape Arago lighthouse (43.4°N, 124.4°W; Station CARO3) and (c) near the EU line at the St George buoy (41.0°N, 124.4°W; NOAA buoy no. 46027). The R/V *Wecoma* cruise is indicated by a thin line in all panels and the approximate time of sampling along GLOBEC lines in the vicinity of each wind station is indicated by initials along this line. The time of the detailed transects in the vicinity of each wind station (TR1, TR2 and TR3; see Figure 1), is indicated by a bold line and numeral in each panel. Note that TR1, along the CR-line, is located between the FM and the EU lines and TR2 is between the NH and FM lines.

Figure 3: Surface-water properties measured off Oregon during July 3-8, 1999. (a) Temperature (°C), (b) salinity (psu) and (c) chlorophyll *a* ($\mu g\ l^{-1}$, estimated from *in-*

vivo fluorescence) were measured continuously while the ship was underway. (d) Silicate (silicic acid) was measured in discrete, acid-preserved samples in the laboratory. Where transects were covered twice during the cruise the later data are plotted over the earlier data. Note the logarithmic color scale used for chlorophyll *a* and silicate concentrations. Contour lines represent the 50, 200 and 1000 m isobaths.

Figure 4: Surface-water concentrations of (a and b) nitrate + nitrite (N) (μmol l^{-1}) and (c and d) iron (nmol l^{-1}) off Oregon, July 3-8, 1999 measured in (a and c) discrete, acidified (pH 2) samples collected from the underway pumping system or surface rosette samples and (b and d) at sea by flow injection analysis, without filtration or acidification. Note the logarithmic color scale. Grey circles in (c) indicate the location of CTD stations where vertical profiles of N and Fe were obtained.

Figure 5: A comparison for (a) N and (b) Fe between measurements made underway by flow injection analysis on an unacidified sample stream and measurements from discrete bottle samples collected from the underway stream and stored acidified at pH 2 for 7 months prior to analysis. The1:1 line is drawn for reference. Note the semi-log scale in (b). Samples with chlorophyll a > 10μg l^{-1} are in filled circles.

Figure 6: Scatter plot of surface salinity versus underway (a) nitrate + nitrite (N) and (b) Fe; (c) scatter plot of underway N versus underway Fe.

Figure 7: Vertical profiles of density anomaly (σ_θ; kg m^{-3}), nitrate + nitrite (N) (μmol l^{-1}), chlorophyll *a* (μg l^{-1}), and dissolvable iron (dFe) (nmol l^{-1}) at the offshore (open symbols and thin lines) and nearshore (closed symbols, thick lines) ends of the lines sampled in July 1999. The offshore dFe profiles are re-plotted in the last panel to enlarge the scale. Station lines are presented top to bottom from north to south, with station locations shown in Figure 3c. On the NH and HH lines chlorophyll *a* was estimated from *in-vivo* fluorescence using the relationship between fluorescence and extracted chlorophyll *a* derived from all other casts. In general, less than 20 hours separated sampling the offshore and the nearshore stations, except along the NH line, where the offshore station was sampled 4 days before the nearshore station.

Figure 8: Vertical profiles of dissolvable iron (dFe) (nmol l^{-1}), fluorescence (Volts), beam attenuation (m^{-1}) and (d) beam attenuation corrected for chlorophyll, from stations at 9 km (thin line, open symbols) and 5 km (thick line, filled symbols) from shore along the NH line.

Figure 9: Underway measurements of the photosynthetic competency parameter, Fv/Fm as a function of local time. FRRf data collected every 4 minutes have been smoothed with a 20 minute running average.

Figure 10: The cross-shelf distribution of (a) N (underway), (b) Fe (measured underway), (c) dFe (measured in discrete acidified samples) and (d) underway Fv/Fm measured at night (between 21:00 and 05:00) during the July 1999 survey.

Figure 11: Transects TR1 (black circles), TR2 (white circles) and TR3 (black squares) showing surface-water properties measured underway in July, 1999: Chlorophyll *a* ($\mu g\ l^{-1}$) was derived from *in-vivo* fluorescence. For locations see dark bars in Figures 1 and 3. Analyses from discrete samples along these transects are presented in Table 2.

Figures

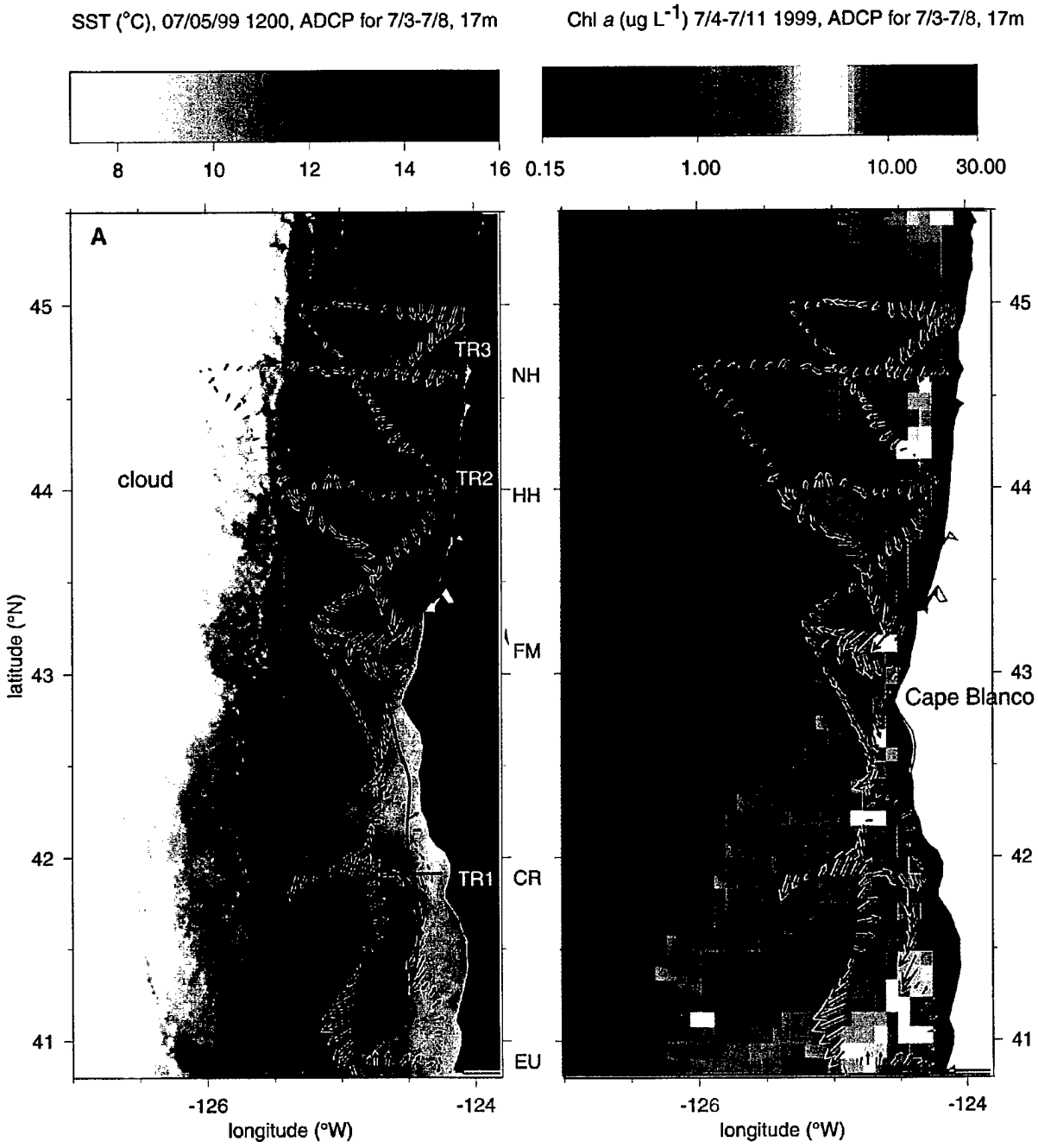

Figure 1

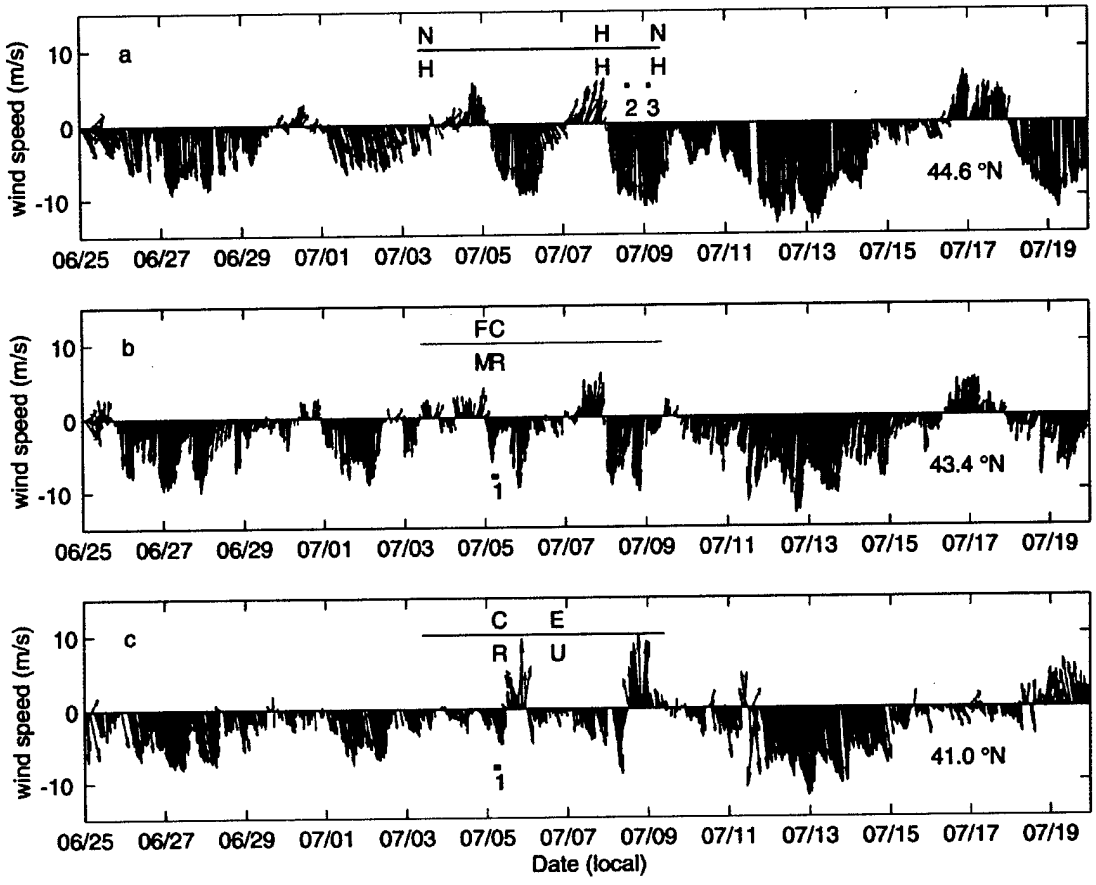
a
N
H
H
N
H
H
2 3
44.6 °N
b
FC
MR
1
43.4 °N
c
C
E
R
U
1
41.0 °N
wind speed (m/s)
10
0
-10
06/25
06/27
06/29
07/01
07/03
07/05
07/07
07/09
07/11
07/13
07/15
07/17
07/19
Date (local)

Figure 2

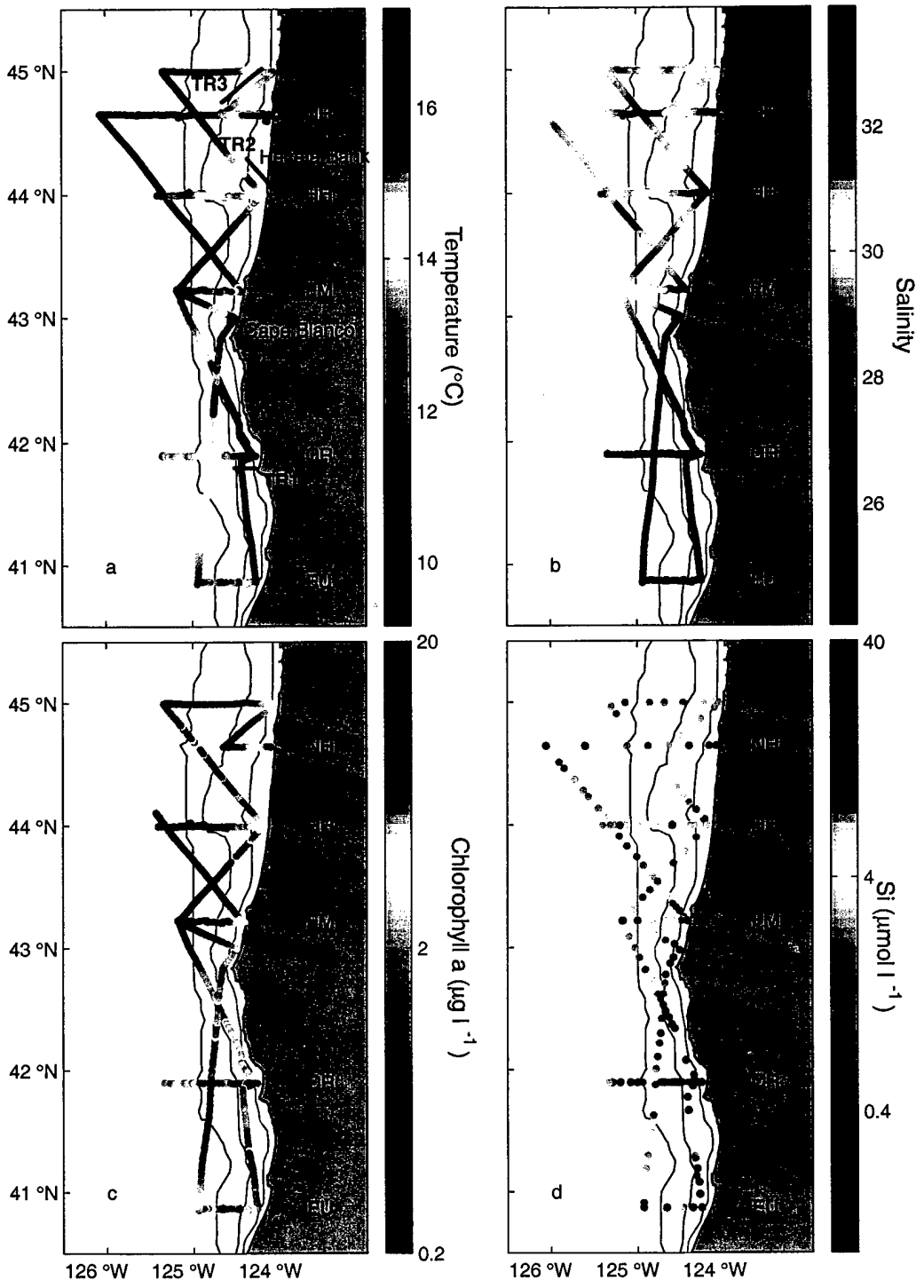
45 °N
44 °N
43 °N
42 °N
41 °N
TR3
TR2
Cape Blanco
a
b
c
d
16
14
12
10
Temperature (°C)
32
30
28
26
Salinity
20
2
0.2
Chlorophyll a (µg l-1)
40
4
0.4
Si (µmol l-1)
126 °W
125 °W
124 °W

Figure 3

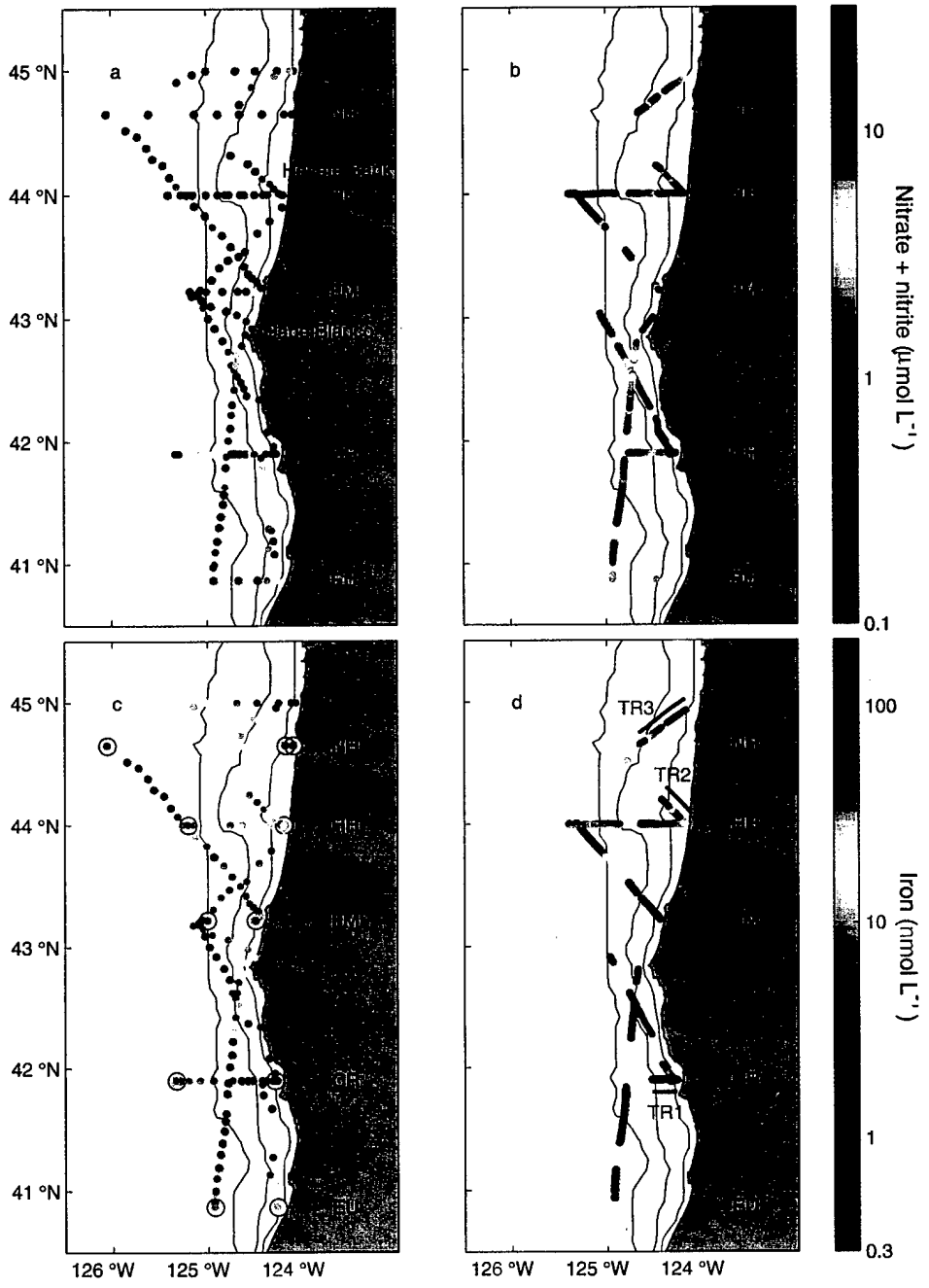
a
b
c
d
45 °N
44 °N
43 °N
42 °N
41 °N
126 °W
125 °W
124 °W
TR3
TR2
TR1
10
1
0.1
Nitrate + nitrite (µmol L⁻¹)
100
10
1
0.3
Iron (nmol L⁻¹)

Figure 4

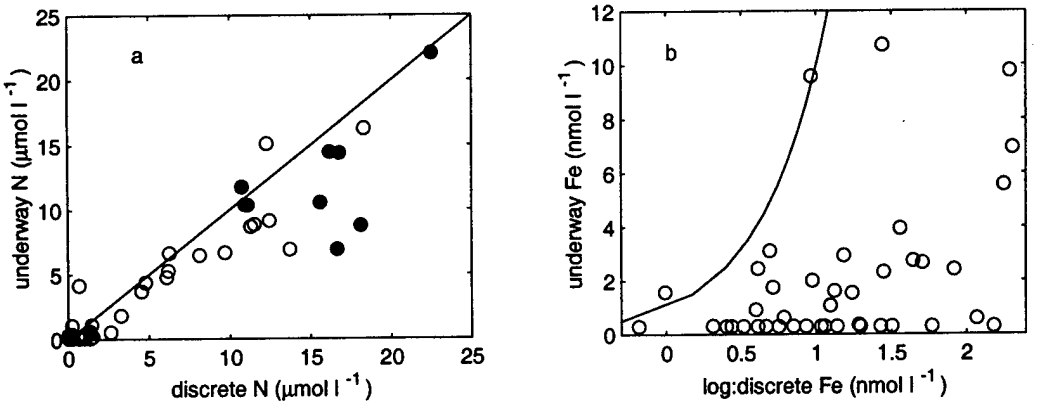

Figure 5

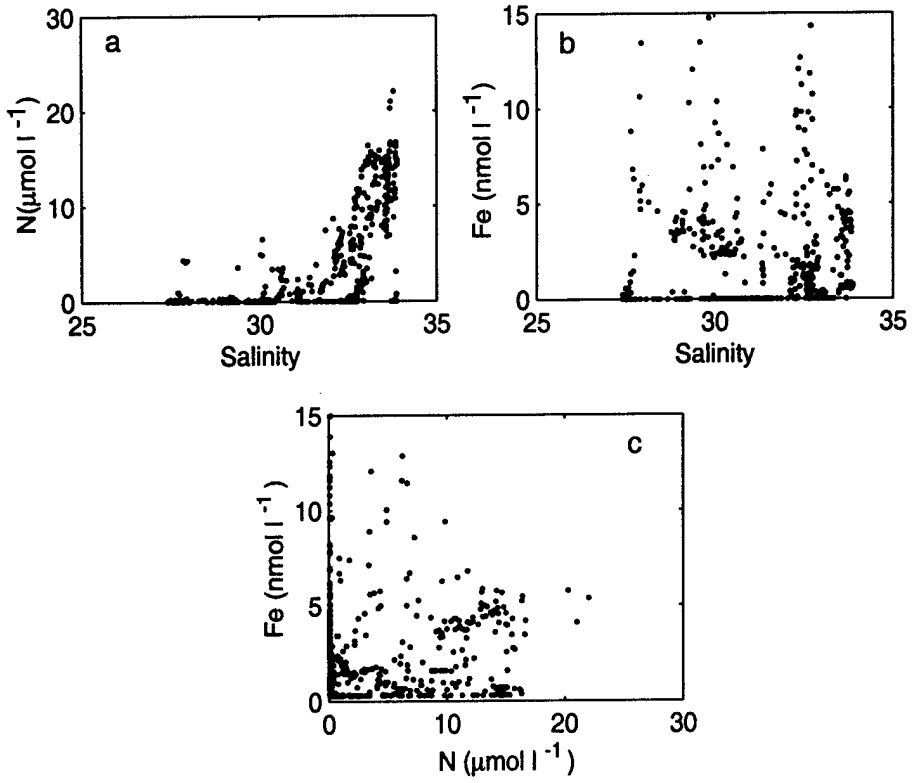

Figure 6

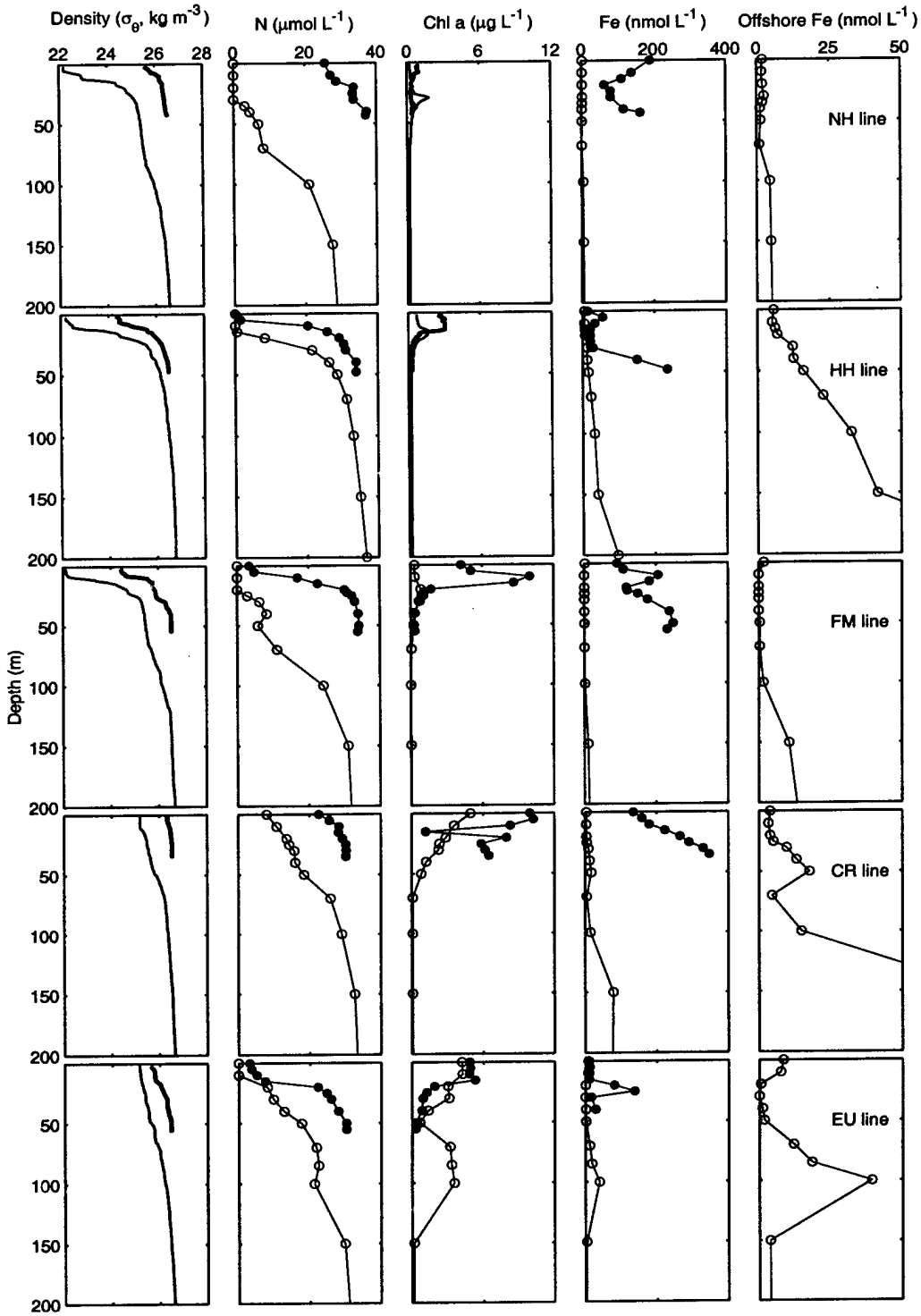
Density (σ_θ, kg m^{-3})
N (μmol L^{-1})
Chl a (μg L^{-1})
Fe (nmol L^{-1})
Offshore Fe (nmol L^{-1})
22 24 26 28
0 20 40
0 6 12
0 200 400
0 25 50
Depth (m)
0 50 100 150 200
NH line
HH line
FM line
CR line
EU line

Figure 7

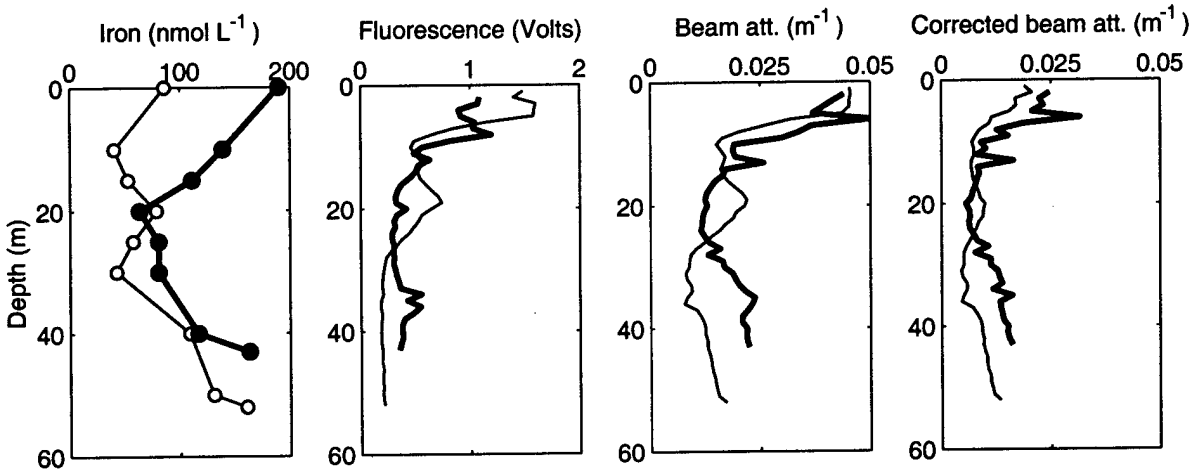

Figure 8

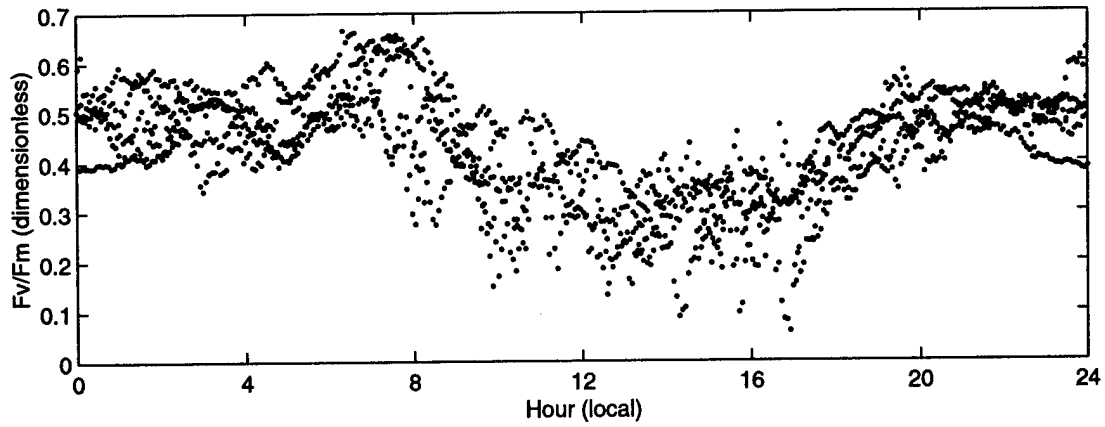

Figure 9

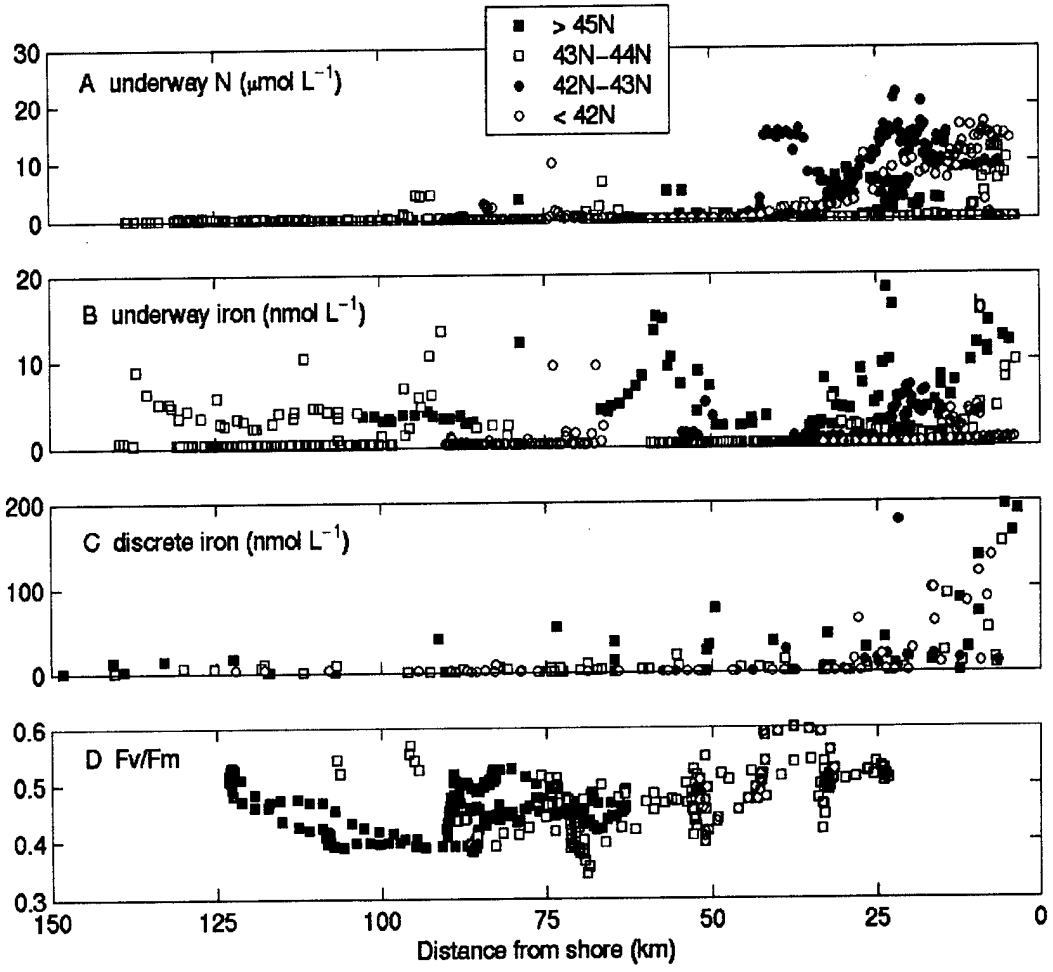
> 45N
43N–44N
42N–43N
< 42N
A underway N (μmol L⁻¹)
B underway iron (nmol L⁻¹)
C discrete iron (nmol L⁻¹)
D Fv/Fm
Distance from shore (km)

Figure 10

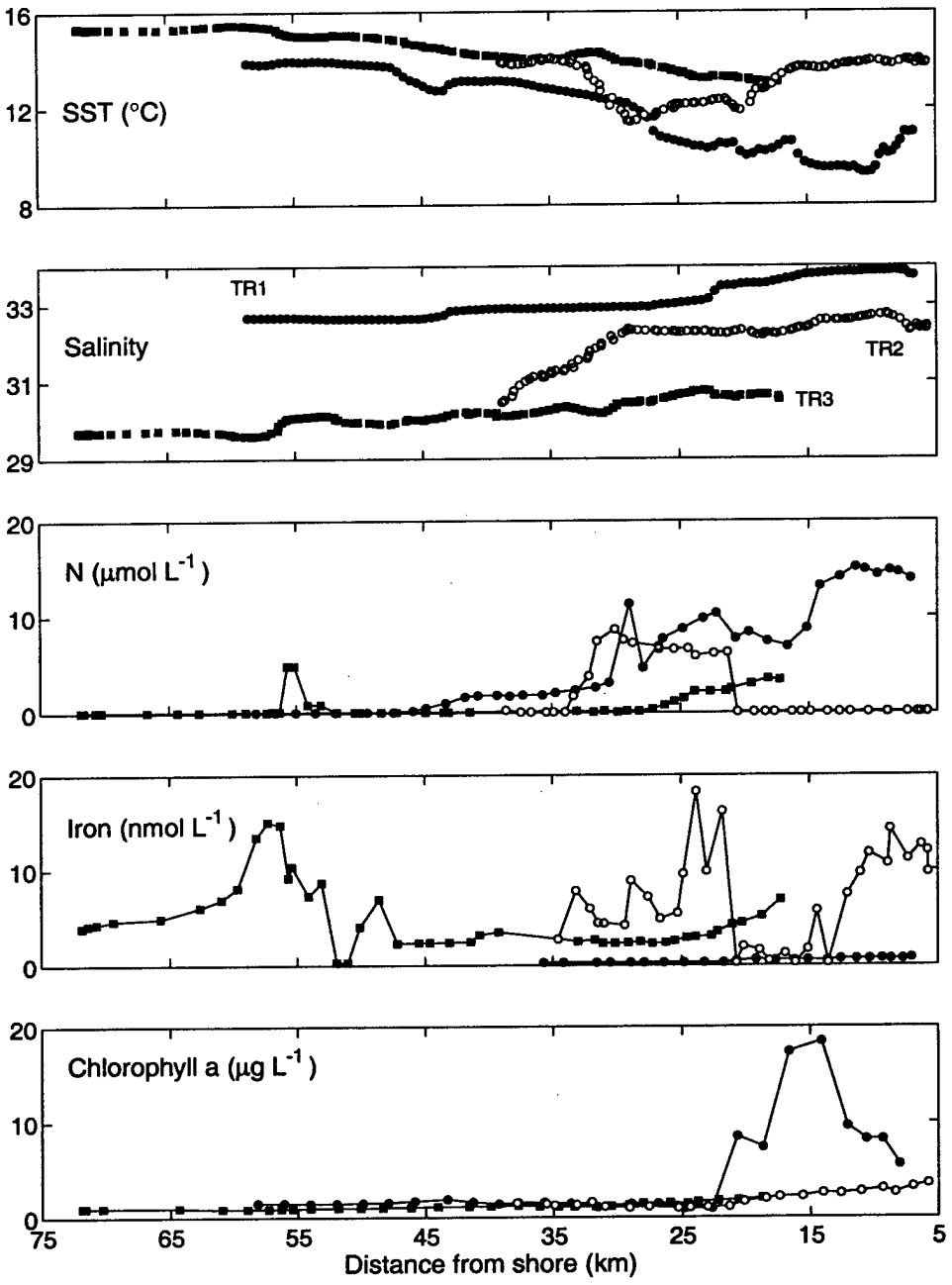
16
12
SST (°C)
8
TR1
33
Salinity
TR2
31
TR3
29
20
N (μmol L-1)
10
0
20
Iron (nmol L-1)
10
0
20
Chlorophyll a (μg L-1)
10
0
75
65
55
45
35
25
15
5
Distance from shore (km)

Figure 11